06,08

Diffusional-deformational instability of the piezoelectric ceramics surface under repeated exposure to gas plasma flow

© K.L. Muratikov, A.A. Kapralov, G.Yu. Sotnikova, A.A. Sukharev

Ioffe Institute,
St. Petersburg, Russia

E-mail: klm.holo@mail.ioffe.ru

Received October 22, 2025
Revised October 22, 2025
Accepted December 27, 2025

The experimental results of the piezoelectric ceramic materials surface modification under the exposure to pulsed high-energy gas plasma flows are presented. Within the boundaries of the diffusional-deformational instability theory, a model, describing processes responsible for the surface deformation and volumetric polarization decrease under increasing plasma loads, is suggested. The dynamic surface equations, accounting for the existence of significant defects concentration gradients as well as the defects activation energy changes in the areas exposed to a high-energy plasma flow, are considered. The estimates of the resulting deformation and surface spatial scale obtained from the suggested model are in good agreement with the experimental data for the piezoelectric ceramic samples exposed to different ion composition plasma flows and qualitatively explain the observed changes in the polarization across the samples volume.

Keywords: piezoelectric ceramics, surface deformation, plasma-surface interaction, instability, defects.

DOI: 10.61011/PSS.2026.02.63384.292-25

1. Introduction

Piezoelectric ceramics belong to the class of functional materials with unique properties of mutual conversion of electrical and mechanical energy due to the direct and reverse piezoelectric effect. The economic efficiency and flexibility of ceramic manufacturing technology in terms of changing its composition make it possible to optimize its functional parameters for specific applications, resulting in its widespread use as a base material for ultrasonic transducers, sensors of various physical quantities, as well as precision actuators and piezoelectric motors [1]. In recent years, there has been a great rise of studies on the synthesis of new promising piezoceramic materials. At the same time, research aimed at improving the long-term stability and resistance of piezoelectric elements performance to external impacts is of the greatest relevance [2,3]. In this regard, the analysis of changes in the material structure impacted by the extreme external loads is of considerable interest, since it allows not only to gain new knowledge about the mechanisms of aging and fatigue of piezoceramic materials [4], but also to formulate relevant areas for improving their synthesis technologies, e.g., fabrication of promising piezoceramic materials with technologically controlled microstructure [5–7].

Advances in the application of plasma technologies to obtain solid-state materials with specified properties [8] stimulate significant interest in using similar approaches to modify the properties of piezoelectric ceramics. In particular, it opens up the possibility of creating compounds and structures in the near-surface layers of piezoelectric materials that are not limited by equilibrium thermodynamics, that is, they are not deployed in standard technological processes. Such microstructuring of the materials surface without significant changes in their bulk properties contributes, for example, to the formation of heat-protective (thermal barrier, TB) layers up to 500 μm thick, which have low thermal conductivity and high resistance to thermal shock. Along with that, the layer's microstructure parameters (thickness, porosity) have a critical effect on its thermal insulation properties [9–11], and also helps to reduce mechanical stresses that occur during thermal cycling, which, in turn, leads to a noticeable increase in service life.

So far, a number of theoretical models have been developed describing changes in the material surface and related functional properties of various materials [12–18]. They analyze processes of various physical nature that develop on the surface of solids under thermodynamic instability caused by various external impacts (laser radiation, ion beams, plasma), leading to rapid (fractions of microseconds) heating of the crystal lattice followed by rapid melting and recrystallization of the surface layer [12–15]. In particular, the possibility of a controlled modification of surface and creation of various structures on it, both of macro- [14] and micro- and nanoscale, is demonstrated [18]. For metals and semiconductors, a theory of electrocapillary instability of the surface layer in the electric field of a laser torch plasma is being developed, describing structural and phase changes in the near-surface layers accompanied by corresponding forms of deformation, including the formation of nanoscale waves, protrusions, or even surface breaks. The phenomenological theory of the formation of self-organizing nanoscale patterns on the surface of crystalline structure of metals and semi-

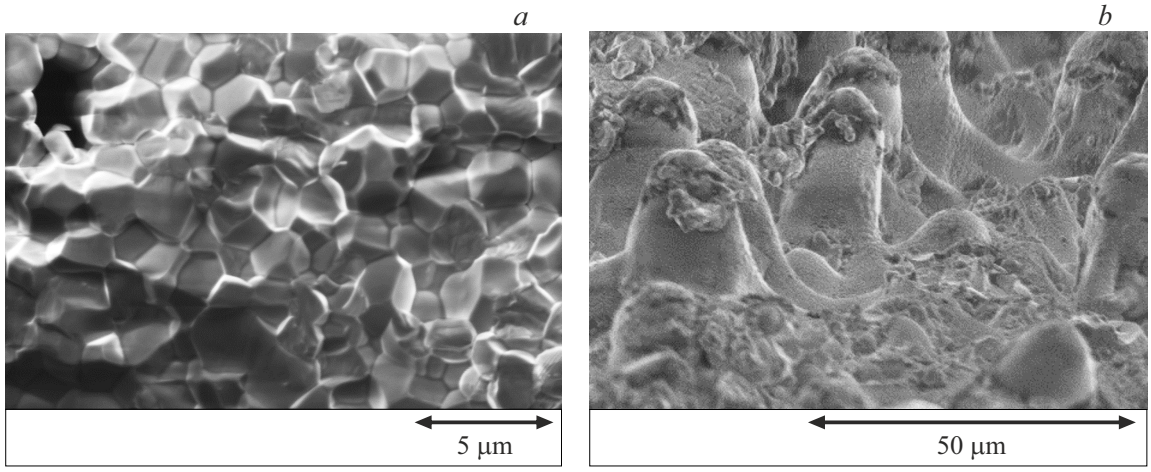

Figure 1. SEM images of the microstructure of the initial (a) and exposed to 20 pulses of hydrogen plasma (b) surface of the piezoelectric ceramics CTSNV-1 fabricated by scanning electron microscopy.

conductors under broad ion beam bombardment, based on thermally activated processes of defect formation, diffusion, and subsequent annealing under stationary conditions, is presented in the study [18].

Unlike metals and semiconductors, experimental data and the results of similar studies for piezoelectric ceramic materials are practically absent. At the same time, the problem of thermal stability of piezoelectric ceramics is one of the key issues in the design and application of piezoelectric devices capable of operating in a wide temperature range, which stimulated our research in this field. An additional incentive for such research is the study carried out at Ioffe Institute related to the prospect of using active piezoelectric elements as part of diagnostic equipment for the International Thermonuclear Experimental Reactor (ITER) [19].

The studies [20,21] outline an experimental setup, a set of measuring techniques, and the first results of a study of the effect of multipulse exposure by high-energy plasma flows on the phase-structural parameters of the surface and a complex of volumetric electrophysical properties of piezoelectric ceramics based on a system of solid solutions of lead zirconate-titanate (PZT, $Pb(Ti_{1-x}Zr_x)O_3$). Currently, these compounds are among the best, most widely used piezoelectric materials and are characterized by significant piezoelectric modules and electromechanical coupling coefficients [22], but with a limited operating temperature range depending on Curie temperature $T_c \leq 300\,^{\circ}C$. Quite unexpected results were obtained in [20,21], evidencing a slight decrease during initial exposure (up to 10 pulses) and further retaining of the volumetric dielectric, piezoelectric and electroacoustic properties of piezoceramics of CTS-19 and CTSNV-1 types up to 70 pulses of plasma exposure, despite exceptionally high thermal loads when the temperature on the material surface during the pulse (of about $20\,\mu s$) reached $1000-1500\,^{\circ}C$. This is more than 3 times higher than the maximum operating temperatures of the studied samples. The observed effect was accompanied by the formation of a quasi-periodic relief on the surface of the samples with typical dimensions of $10-20\,\mu m$. This allowed to assume that plasma exposure triggers processes on the ceramic surface leading to its modification, which raises the material thermal stability. In this regard, the main purpose of this study is to develop a physical model for the formation of relief (plastic deformation) of the surface layer of piezoelectric ceramics impacted by a pulsed plasma load.

2. Experiments on formation of the surface relief of piezoelectric ceramics impacted by a pulsed plasma flow

Figure 1 illustrates the microstructure of a ceramic surface fabricated using standard technology at „Aurora-Elma“ enterprise (Volgograd, Russia) before (a) and after (b) exposure to 20 pulses of the hydrogen plasma.

The impact parameters correspond to the parameters of the coaxial plasma accelerator [23] and the configuration of experimental setup [20,21], which provides a dosed pulse effect from the gas plasma with variable ion composition and an energy of $\sim 0.1\,MJ/m^2$ (current flow density $\sim 10^{21}\,m^{-3}$, duration of the plasma pulse exposure $20\,\mu s$, heat load factor $F_{HF} \approx 20\,MW/(m^2 \cdot \sqrt{s})$). Analysis of the temperature variation in the irradiated surface of samples recorded using a high-speed two-spectral photodiode pyrometric sensor [24], showed that its maximum value lies within the range of $1000-1200\,^{\circ}C$ and depends little on composition of the plasma-forming gas.

As seen from the Figure 1, on the surface of initial (non-irradiated) sample of CTSNV-1 piezoceramics distinguished by relatively closely packed multi-facet grains of the

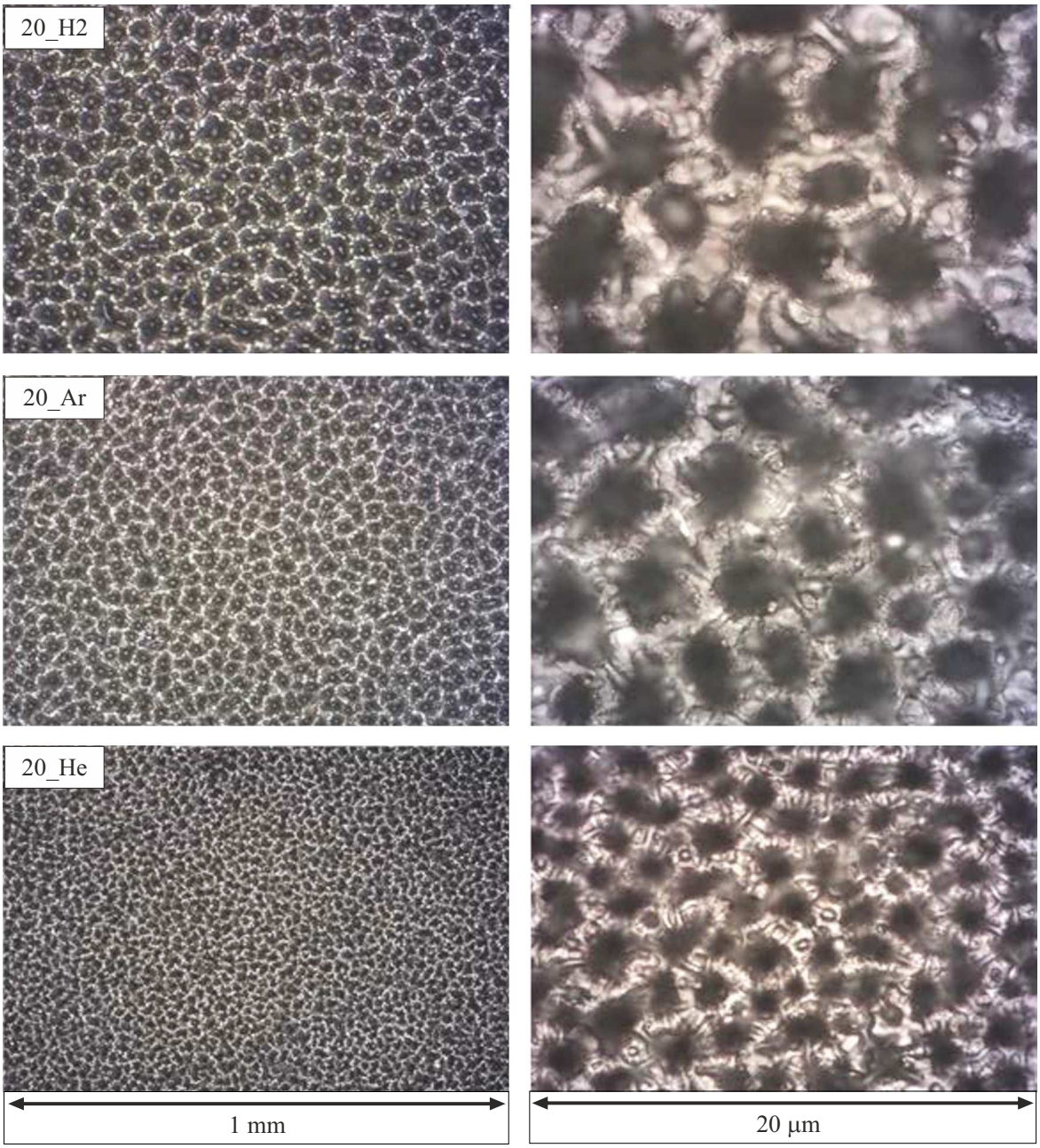

Figure 2. Optical images of the surface of CTSNV-1 piezoelectric ceramic samples after treatment by 20 pulses of hydrogen (20 H2), helium (20 He) and argon (20 Ar) plasma, with varying magnification.

piezoelectric material about $2-5\,\mu$m (Figure 1, *a*), a clearly distinct „columnar" structure with typical sizes of $20\,\mu$m is formed. The quasi-periodic structure of the observed relief is seen in Figure 2, which shows optical images of CSTNV-1 ceramic samples surface irradiated with pulsed flows of helium (He), hydrogen (H2) and argon (Ar) plasma, i. e. plasma with significantly different properties of its constituent particles. There is a qualitative similarity of the relief on the surface of piezoceramics, formed as a result of the same dose of exposure to gas plasma of different ionic composition.

3. Theoretical model of the surface relief formed in piezoelectric ceramics impacted by a pulsed plasma flow

Let us analyze the formation of the surface relief of piezoelectric ceramics from the standpoint of irreversible (plastic) deformation occurring as a result of external forces, under which irreversible displacement of interatomic bonds takes place. The nature of plastic deformation depends on the temperature, the duration of the load and the rate of deformation. The energy introduced into a solid by high-

intensity (dense) gas plasma flows is consumed by the processes of high concentration radiation defects (vacancies and interstitial atoms) formation in its thin surface layer, thus allowing to consider the process of surface relief formation in piezoelectric ceramics from the standpoint of the diffusional-deformational instability theory [14]. In this theory, it is assumed that defects form in the medium under external impacts in accordance with a certain nonlinear law. The tensor of mechanical stresses in a piezoelectric material during the generation of defects in it, taking into account the effects of elevated temperature, is described by the expression [25]:

$$\sigma_{ij} = \sigma_{ij}^{(0)} + C_{ijkl}(\Omega_{kl} n - \alpha_{kl} T), \tag{1}$$

where tensor $\sigma_{ij}^{(0)} = C_{ijkl}\varepsilon_{kl}$ — describes the purely elastic properties of a piezoelectric material, C_{ijkl} is the tensor of its elastic modulus, Ω_{kl} is a tensor describing the behavior of the defect's activation volume, n — defects concentration, α_{kl} — tensor of thermal expansion coefficient of the piezoelectric material.

The simultaneous dependence of the material stress tensor on the defect concentration and the defect concentration on temperature can lead to the development of diffusional-deformational instability in it [25], the analysis of which is generally based on a system of equations binding the piezoelectric deformation and the processes of generation and kinetics of defects in it. When considering the kinetics of defects in the diffusional approximation, this system can be written as:

$$\rho \frac{\partial^2 u_i}{\partial t^2} = \frac{\partial \sigma_{ij}^{(0)}}{\partial x_j} + C_{ijkl}\left(\Omega_{kl} \frac{\partial n}{\partial x_j} - \alpha_{kl} \frac{\partial T}{\partial x_j}\right), \tag{2}$$

$$\frac{\partial n}{\partial t} = D_{il} \frac{\partial^2 n}{\partial x_i \partial x_j} \Delta n - \frac{1}{\tau}\left[n - n_0 \exp\left(-\frac{E_a}{k_b T}\right)\right] + G_N, \tag{3}$$

where ρ — density of the medium, μ_i — components of the displacement vector of the medium during deformation, D_{ij} — tensor of the diffusion coefficient of defects, τ — defect relaxation time, n_0 — initial defect concentration, G_N — defect generation rate as a result of external impact, E_a — activation energy of defect formation, k_b — Boltzmann constant.

Equation (3) assumes that the excitation of defects is quasi-equilibrium in nature and evolves according to Arrhenius law. The equations (2) and (3) should be considered as a nonlinear system of equations, since the generation of defects leads to a modulation of their activation energy in accordance with the ratio [25]:

$$E_a = E_a^{(0)} + \theta_{ij} u_{ij}, \tag{4}$$

where θ_{ij} is the strain potential tensor, $E_a^{(0)}$ is the activation energy of the defect in the absence of deformation.

The use of the system of equations (2)–(4) makes it possible to determine the conditions for development of instabilities in the material under external influence. To simplify further assessment of the conditions of instability formation, we assume that the anisotropy of the material is small, i.e. $C_{ijkl} \cong C\delta_{ik}\delta_{jl}$, $\Omega_{ij} \cong \Omega\delta_{ij}$, $D_{ij} \cong D\delta_{ij}$, $\theta_{ij} \cong \theta\delta_{ij}$. To analyze the system behavior, we assume that in the initial state it is in a certain equilibrium state $\mathbf{u} = \mathbf{u}_0$, $n = n_0$ at a given temperature and introduce some small disturbance into it in accordance with the equalities $\mathbf{u} = \mathbf{u}_0 + \mathbf{u}_1$, $n = n_0 + n_1$, where $\mathbf{u}_1 = \mathbf{u}_\kappa e^{\gamma t + i\mathbf{kr}} + \text{const}$, $n_1 = n_\kappa e^{\gamma t + i\mathbf{kr}} + \text{const}$. We linearize the system of equations (2)–(4) with respect to small perturbations. Then, given that formation of defects with a concentration of n and an activation volume of Ω introduces deformation Ωn into the medium, the deformation addition to the activation energy can be transformed to $\theta_{ij} u_{ij} \cong \theta\Omega n$. Then, from equation (3) we'll get the dispersion equation:

$$\gamma = -Dk^2 - \frac{1}{\tau}\left(1 + N_0 \frac{\theta\Omega}{k_b T}\right), \tag{5}$$

where

$$N_0 = n_0 \exp\left(-\frac{E_a^{(0)}}{k_b T}\right)$$

— initial equilibrium value of the vacancies concentration. According to equation (5), the values of $\gamma < 0$ correspond to the stable development of the system, while the values of $\gamma > 0$ lead to instability. Given that $\theta > 0$, then in accordance with (5) for defects with $\Omega > 0$, the system evolution always occurs according to the stable scenario. However, for vacancies characterized by values of $\Omega < 0$, conditions for the development of instability may arise. When exposed to plasma, vacancies and interstitial atoms are formed within the solids. The latter move faster and can come to the surface or join other defects, contributing to the accumulation of vacancies across the material [25]. In this case, when the vacancy concentration becomes greater than a certain critical value, the system will become unstable. In accordance with equation (5), for this, the vacancy concentration shall satisfy the condition:

$$N_0 \geq N_c = \frac{k_b T}{\theta|\Omega|}(Dk^2\tau + 1), \tag{6}$$

where N_c is a certain critical value of the vacancy concentration at which instability begins to develop. In accordance with (6) at $N_0 \cong N_c$

$$k^2 = \frac{1}{D\tau}\left(N_c \frac{\theta|\Omega|}{k_b T} - 1\right). \tag{7}$$

From the ratio (7) It follows that the condition $N_c \frac{\theta|\Omega|}{k_b T} \geq 1$ shall be fulfilled in order for instability to develop in the area of the gas plasma pulse. The values of θ and Ω parameters are specific to a particular piezoelectric material and are not given in the literature. Let us perform numerical estimates of the critical vacancy concentrations using the given values $\theta \approx 10\,\text{eV}$ [14,26] and $\Omega \approx 10^{-23}\,\text{cm}^3$ [27]. Calculations

show that at a temperature of $T \approx 10^3$ K, the deformation occurrence condition is satisfied when the vacancy concentration exceeds the value of $N_c = \frac{k_b T}{\theta|\Omega|} \approx 10^{21}\,\text{cm}^{-3}$, which is quite achievable, given that the equilibrium vacancy concentration for piezoelectric PZT ceramics is $\sim 10^{19}\,\text{cm}^{-3}$ [4]. For these ceramic materials the vacancy concentrations $N_0 \geq N_c$ correspond to the deformation values of $10^{-3}-10^{-2}$, which is close to the critical level at which plastic deformation occurs. Such deformations occur in the near-surface area of ceramics, where the highest temperature values are reached.

Obviously, the physical parameters of ceramic grains have a certain variation, therefore, during the first plasma pulses, instability will develop in grains with the lowest N_c. During rapid surface cooling, some of the formed point defects do not have time to reach an equilibrium state, and additional frozen nonequilibrium vacancies will appear in the surface layer. When subsequent plasma pulses arrive, as vacancies accumulate, the surface relief will form near other grains as well.

To qualitatively explain the mechanism of relief formation and assess its quantitative parameters, let us consider in more detail the time behavior of the volumetric force included in the motion equation (2) and acting in a direction perpendicular to the surface. According to the right-hand side of the equation (2) the volumetric force consists of two components — concentrational and thermal (thermoelastic). During the plasma pulse impact, the ceramics surface temperature rises and the vacancy concentration goes up. In this case, the directions of action of both forces in the ceramics surface layer coincide and contribute to its rise. Thus, the surface in the instability zone will experience accelerated movement. After the pulse ends, the surface will still remain hot, however, it will begin to cool rapidly due to the radiation mechanism. In these conditions, the temperature gradient near the surface will change sign, but the sign of the concentration gradient will remain the same. As a result, the force thermoelastic component will counteract the force caused by the vacancy concentration gradient. At a certain point in time, these two forces will compensate for each other and the accelerated movement of the surface will stop. Assuming that instability growth stops when these forces are equal at some point $t = t_0$, then the resulting typical size of the relief heterogeneity can be estimated from the condition:

$$|\Omega| \left.\frac{\partial n}{\partial z}\right|_{t=t_0} \approx \alpha_T \left|\frac{\partial T}{\partial z}\right|\Big|_{t-t_0}, \qquad (8)$$

where α_T — thermal expansion coefficient of ceramics (z axis is directed perpendicular to the surface).

We assume that the main drop in vacancy concentration occurs at a distance of L, commensurate with the inhomogeneity size, and the major temperature change in the surface layer occurs at the diffusion penetration depth of the heat wave $L_D = \sqrt{\chi\tau}$, where χ — thermal diffusivity coefficient, τ — duration of heat exposure pulse. Expression (8) may be transformed to

$$|\Omega| \frac{\Delta N_0}{L} \approx \alpha_T \frac{\Delta T}{L_D},$$

from which we may assess the resulting typical size of inhomogeneities

$$L \approx \sqrt{\chi\tau} \cdot |\Omega| \frac{N_0}{\alpha_T \Delta T}, \qquad (9)$$

With the exposure pulse duration of $20\,\mu$s, leading to the surface heating up to $\Delta T \approx 10^3$ K, growth of vacancies concentration up to $N_c \approx 10^{21}\,\text{cm}^{-3}$ and using PZT-ceramics typical coefficients of thermal diffusivity $5 \cdot 10^{-7}\,\text{m}^2/\text{s}$ [28] and heat expansion at high temperature of $\alpha_T = 8 \cdot 10^{-6}\,\text{K}^{-1}$ [29], we'll get the value of $L \approx 4\,\mu$m for the inhomogeneity resulting typical size.

Expression (9) gives a functional relationship between the size of the inhomogeneities and the parameters of the piezoceramic material (Ω, χ, α_T) and plasma exposure ($\tau, \Delta N_c, \Delta T$). The value $L \approx 4\,\mu$m for the vacancy concentration $N_0 = N_c \approx 10^{21}\,\text{m}^{-3}$ is in good accordance with the average ceramic grain size of $5\,\mu$m (Figure 1, *a*), but 3–5 times smaller than the sizes of the inhomogeneities observed in the experiment and shown in Figure 1, *b*) and in Figure 2. At the same time, it follows from (9) that exceeding the value of the defect concentration on the surface of the irradiated sample N_0 of the critical concentration N_c by only 3–5 times allows not only to reconcile theoretical estimates with experimental ones, but also to explain the observed difference in the surface structure by various mechanisms of defect formation when irradiated with plasma with a different particle composition.

4. Analysis of changes in piezoelectric ceramics impacted by a pulsed plasma flow

Unsteady deformations in the piezoceramic sample surface layer exposed to a plasma pulse lead to the excitation of acoustic pulses in its volume, that is, the generation of gradually attenuating acoustic waves with a wide range of frequencies. The presence of a piezoelectric effect, in its turn, will lead to the excitation of an alternating electric field in it with a consistently decreasing amplitude. With the considered level of deformations $10^{-3}-10^{-2}$ and sufficiently high values of piezoelectric modules (in particular, for the considered ceramics CTSNV-1 and CTS-19 $d_{33} \approx 300 \cdot 10^{-12}$ K/N), the amplitude of electric field oscillations may reach 6 MV/m, which is close to the upper limit (10 MV/m) of the local depolarization fields of ferroelectric materials [4] and may cause gradual depolarization of ceramic samples with a higher number of plasma exposure pulses. The phenomenon of depolarization of piezoceramic material after several cycles of applied alternating field with a successively decreasing amplitude

from 20 to 2 MV/m in ten steps was analyzed in [30] based on the concept of Preisach dipolar unit model, the central point of which is the assumption of the presence of the field distribution switches for ceramic grains with different initial polarization. In this regard, the analysis of changes in the polarization state after exposure to plasma pulses is of considerable interest. Microscopic fatigue models of piezoelectric materials [31,32] have shown that it is the accumulation of oxygen vacancy defects in ferroelectric materials of the perovskite structure impacted by a cyclic electric field that make it possible to explain most of the observed aging features of piezoceramic materials [4].

To study the polarization state of the samples, an experimental method was used based on the pyroelectric effect — occurrence of an electric charge on the surface of a polarized piezoceramic sample when its temperature changes, known in the literature as „Laser Intensity Modulation Method" (LIMM) [33]. Theoretical justification of the method and its practical implementation are given in [34,35]. By heating the sample surface using power-modulated laser radiation and changing the modulation frequency, f, data can be obtained on polarization distribution in the piezoceramic sample thickness within the heat wave penetration depth, determined by the ratio $L_D = \sqrt{\chi/\pi f}$, where χ — coefficient of thermal diffusivity. In this experiment, a semiconductor laser with a wavelength of $0.68\,\mu$m and a maximum radiation power of 5 mW was used. The laser radiation modulation frequency varied from 0.5 Hz to 150 kHz, which, at $\chi = 5 \cdot 10^{-7}\,\mathrm{m^2/s}$, makes it possible to analyze the sample's polarization state in the layer thickness from $1\,\mu$m to 0.5 mm (counting from the heated surface) and compare the polarization distribution over the thickness of exposed and non-exposed samples surfaces (the thickness of the samples did not exceed 1 mm with a diameter of 10 mm, electrodes were applied to both surfaces of the samples).

Figure 3 shows the pyroelectric response (amplitude of harmonic voltage proportional to the charge variation at the sample electrode due to polarization of the heated volume) versus heat wave penetration depth for a non-exposed sample of CTS-19 and samples after exposure to various numbers of hydrogen plasma pulses.

The appearance of a depolarized layer in the near-surface region of the piezoceramic samples on the exposed side is clearly visible. The depth of depolarized layer does not exceed $10\,\mu$m for all exposed samples up to 70 plasma exposure pulses. At the same time, after the first 10 pulses, a certain recovery of the ceramics surface polarization properties was observed. In the ceramic volume, the initial polarization decreased by about 20 % during the first pulses, after which the polarization of the ceramic volume remained almost unchanged for the next several dozen pulses. The observed effect of stabilizing the pyroelectric response after 20 pulses of exposure coincides with the similar effect of „recovery" and stabilization of the main parameters of piezoceramics when exposed to hydrogen and helium plasma up to 70 pulses, first discovered in [21].

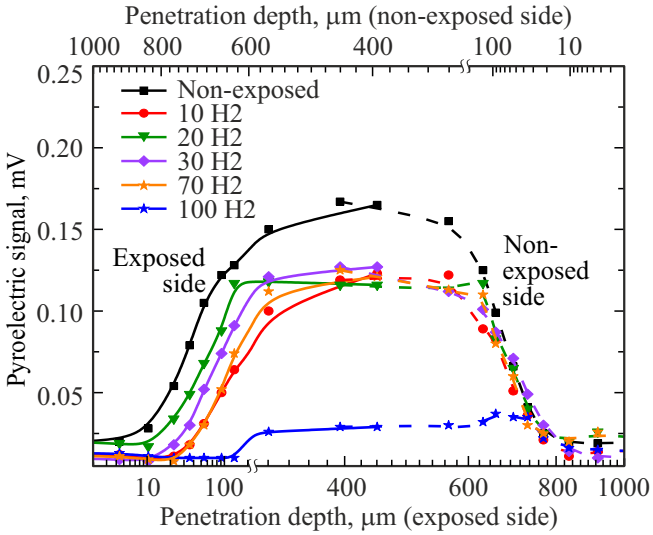

Figure 3. Pyroelectric response of CTS-19 samples depending on the heat wave penetration depth for the non-exposed samples and samples exposed to 10 (10 H2), 20 (20 H2), 30 (30 H2), 70 (70 H2) and 100 (100 H2) hydrogen plasma pulses with a heat flow factor $F_{\mathrm{HF}} = 20\,\mathrm{MW/(m^2 \cdot \sqrt{s})}$.

A drop in the volumetric polarization of ceramics was observed with a pulse count of about one hundred. This behavior of the volumetric piezoelectric properties of PZT ceramics, depending on the number of plasma pulses, is in good agreement with Preisach model discussed above and indicates a rather high quality of the material due to a small variation in the polarization angles of individual grains.

The results shown in Figures 1–3 were obtained for industrial samples of PZT piezoceramics fabricated using standard technology of „Avrora-Elma", however, we also studied other types of ceramics, including porous ferro-piezoceramics PCR-1 (samples provided by the Center of Prospective Research and Development at the Southern Federal University, Rostov-on-Don, Russia), close to CTS-19 and CTSNV-1 in terms of the components ratio. The porous piezoceramics PCR-1 (20 % porosity) is distinguished by a random distribution of irregularly shaped pores from 10 to $30\,\mu$m in size inside a piezoceramic carcass of closely-packed grains of a regular multifaceted shape $2-5\,\mu$m in size [36], matching in terms of their parameters with the dense ceramics CTSNV-1 mentioned above (Figure 1, *a*). Figure 4 shows optical images of the surface area of a piezoceramic sample PCR-1 after exposure to 20 pulses of hydrogen plasma.

The overlap of the two relief structures, which have different typical spatial scales, is clearly visible. Obviously, the presence of pores and any other extended defects in the material means that it is heterogeneous on a scale comparable to the size of such defects. For samples of piezoceramics PCR-1, it follows that anisotropy may be expected on a scale of $\sim 50\,\mu$m, which corresponds to the thicknesses of the near-surface layers where visible changes

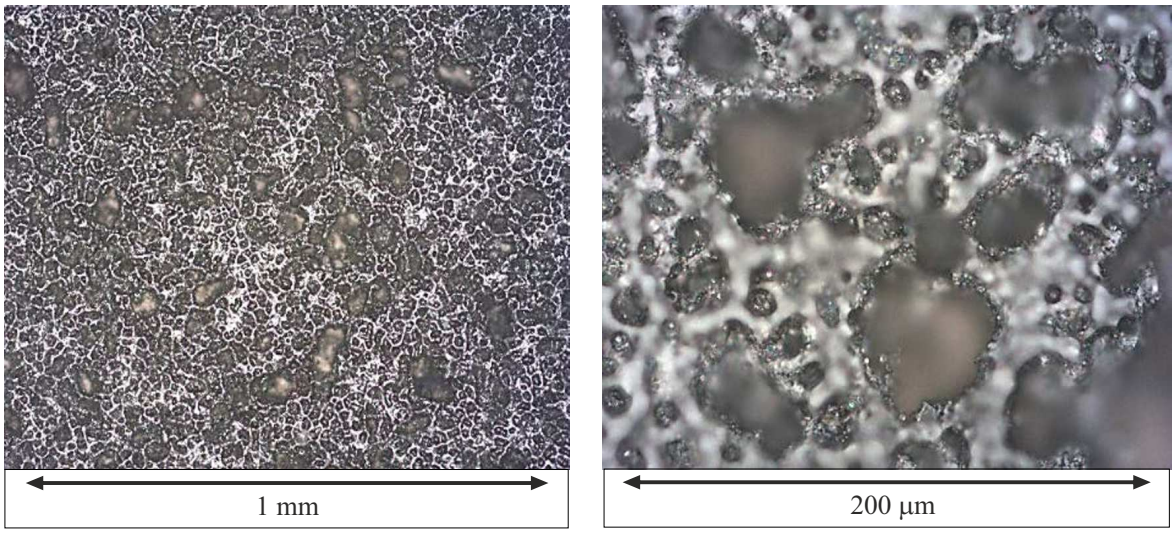

Figure 4. Optical images of an area of porous piezoceramics PCR-1 sample surface (20 % porosity) after exposure to 20 pulses of hydrogen plasma (heat load factor $F_{HF} \approx 20\,MW/(m^2 \cdot s^{1/2})$).

in the material structure are observed, i. e., to the depths of heating to temperatures when a number of vacancies sufficient to initiate the instability are generated. Since the above model deals with the instability evolution in the approximation of an almost isotropic material, its use for anisotropic materials is strictly speaking not correct. However, if the heterogeneity of the material is of an „impurity" type, i. e., the percentage of volume occupied by extended defects is small, then we should expect a similar development of instability, and accordingly, the scale of the relief formed on the surface to be similar to the isotropic material. This is proved by formation of a relief with a typical scale of inhomogeneity $\sim 30\,\mu m$ on the surface of ceramics PCR-1 after plasma exposure, similar to ceramic samples CTS-19 and CTSNV-1 with closely-packed grains of the same size.

At the same time, the observed structure of a smaller scale is probably related to the material anisotropy, and can be described within the framework of additional terms in the model under consideration, which, however, lies outside the scope of this study. It should be noted that the presence of several characteristic scales of heterogeneity in the material surface after plasma exposure may evidence a strong unevenness in defects distribution in the material or deviations of its physical parameters from the declared ones, i. e., a sign of differences/compromised fabrication technology.

Figure 5 shows the results of an experimental study of the nature of the polarization distribution over the volume of a porous piezoceramic sample before and after exposure to 20 pulses of hydrogen plasma. LIMM method was used in experiments, the calculations were performed taking into account the parameters of piezoceramics PCR-1, given in [36,37]. As with closely-packed piezoceramics CTS-19 (Figure 3), the formation of a depolarized layer with a thickness of $\approx 10\,\mu m$ is observed on the exposed side. At the same time, with the same number of pulses of exposure to hydrogen plasma (20 pulses), a stronger decrease in bulk polarization (by more than 30 %) is observed in porous ceramics compared to the CTS-19 sample, which is apparently caused by a decline in coercive field because of specific microstructure of porous piezoceramics [36]. This leads to an accelerated depolarization process of the piezoceramic material during the cyclic application of an alternating field generated by excitation of elastic waves by plasma pulses in its volume at comparable levels of deformation and piezoelectric modulus.

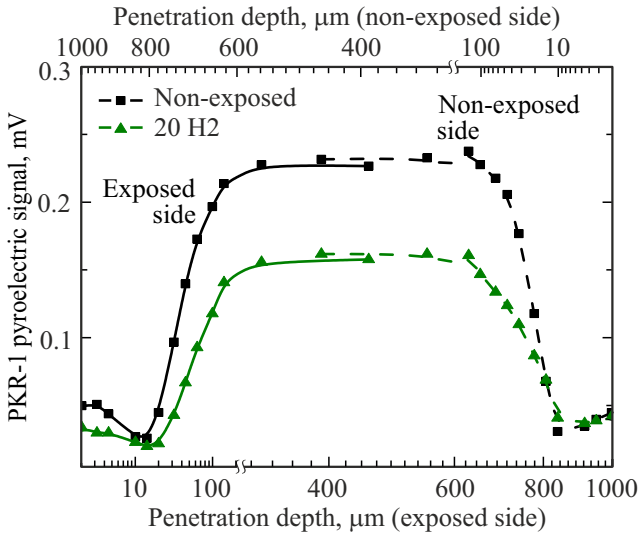

Figure 5. Pyroelectric response of PCR-1 samples depending on the heat wave penetration depth for the non-exposed sample and sample exposed to 20 (20 H2) hydrogen plasma pulses with a heat flow factor of $F_{HF} = 20\,MW/(m^2 \cdot \sqrt{s})$.

5. Conclusion

It was demonstrated that the diffusional-deformational model of unsteady state evolution in a crystalline piezoceramic material exposed to a high-energy plasma load could give a clue to explaining the nature and quantifying the level of elastic and plastic strains that formed the self-organizing structures with typical dimensions $5-20\,\mu$m on the surface of piezoelectric ceramics and resulted in an aggravation of its volumetric polarization properties. The obtained quantitative estimates are in good agreement with experimental data for the closely-packed piezoelectric ceramics CTSNV-1 and CTS-19, which confirms the possibility of using plasma technologies for manufacture of promising piezoceramic materials with technologically controlled microstructure.

Using the samples of porous piezoceramics PCR-1, it is shown that the proposed model may be used to analyze the distribution of defects in ceramic materials made using various technologies and predict the defective structure evolution in the material exposed to external thermal stress, which is of significant fundamental interest for clarifying the physical mechanisms of fatigue and aging of various piezoelectric materials.

Acknowledgments

The authors are grateful to A.V. Ankudinov and A.V. Nashchekin (Ioffe Institute) for the optical and electron microscopy examinations performed on the equipment provided by the Federal Joint Research Center „Material Science and Characterization in Advanced Technology“ and N.A. Shvetsova (Center of Prospective Research and Development at Southern Federal University) for the provided samples of porous piezoceramics.

Funding

The work was partially supported by grant of the Russian Science Foundation No. 24-19-00716 (https://rscf.ru/project/24-19-00716/).

Conflict of interest

The authors declare that they have no conflict of interest.

References

[1] K. Uchino. Advanced piezoelectric materials. Science and Technology (Second Edition). Woodhead Publishing (2017). 830 p.
[2] A.E. Panich. Physicheskie osnovy pryborostroeniya **8**, *1* (31), 30 (2019) (in Russian).
[3] A.Y. Malykhin, L.A. Dykina, E.A. Panich. Russian chemistry magazine **64**, *3*, 97 (2020) (in Russian).
[4] J.A. Genenko, J. Glaum, M.J. Hoffmann, K. Albe. Mater. Sci. Eng. B **192**, 52 (2015).
[5] E. Mercadelli, C. Galasi. IEEE Trans. Ultrason. Ferroelec. Freq. Contr. **68**, *2*, 217 (2021).
[6] A.N. Rybyanets, I.A. Shvetsov, N.A. Shvetsova, M.A. Marakhovsky, N.A. Kolpacheva. J. Adv. Dielectr. **15**, *4*, 2540001 (2025).
[7] N. Shen, Q. Liao, Y. Liao, R. Li, Y. Zhang, S. Song, Y. Song, C. Zhu, L. Qin. Coatings **15**, *1*, 51 (2025).
[8] X. Feng, H. Tao, S. Yang, C. Liu, C. Wei, Y. Wang, H. Zhao, S. Yao, Z. Cheng, Adv. Mater. Technol. **10**, *16*, 240220710 (2025).
[9] N. Curry, M. Leitner, K. Körner. Coatings **10**, *10*, 957 (2020).
[10] O. Aranke, M. Gupta, N. Markocsan, Xin-Hai Li, B. Kjellman. J. Therm. Spray. Tech. **28**, 198 (2019).
[11] S. Tao, J. Yang, W. Li, F. Shao, X. Zhong, H. Zhao, Y. Zhuang, J. Ni, S. Tao, K. Yang. Coatings. **10**, *9*, 894 (2020).
[12] X. Yan, P. Zhai, C. Yang, S. Zhao, S. Nan, P. Hu, T. Zhang, Q. Chen, L. Xu, Z. Li, J. Liu. Appl. Phys. Lett. **125**, *4*, 042103 (2024).
[13] S.A. Akhmanov, V.I. Yemelyanov, N.I. Koroteev, V.N. Seminogov. UFN **147**, 675 (1985) (in Russian).
[14] F.Kh. Mirzoev, V.Ya. Panchenko, L.A. Shelepin. UFN **166**, *1*, 3 (1996) (in Russian).
[15] S.I. Kudryashov, N.A. Smirnov, N.I. Busleev, P.P. Pakholchuk, M.S. Kovalev, M.A. Tarkhov, G.H. Sultanova, I.V. Krasnogorov. Pisma v ZhETF **121**, *9*, 711 (2025) (in Russian).
[16] A.A. Bormatov, V.M. Kozhevin, S.A. Gurevich. ZhTF **91**, *5*, 721 (2021) (in Russian).
[17] V.M. Kozhevin, M.V. Gorokhov, A.A. Bormatov. Pis'ma v ZhTF **43**, *14*, 72 (2017) (in Russian).
[18] R.M. Bradley, D.A. Pearson. Nucl. Instrum. Methods Phys. Res. B **551**, 165345 (2024).
[19] E.E. Mukhin, V.M. Nelyubov, V.A. Yukish, E.P. Smirnova, V.A. Solovei, N.K. Kalinina, V.G. Nagaitsev, M.F. Valishin, A.R. Belozerova, S.A. Enin, A.A. Borisov, N.A. Deryabina, V.I. Khripunov, D.V. Portnov, N.A. Babinov, D.V. Dokhtarenko, I.A. Khodunov, V.N. Klimov, A.G. Razdobarin, S.E. Alexandrov, D.I. Elets, A.N. Bazhenov, I.M. Bukreev, An.P. Chernakov, A.M. Dmitriev, Y.G. Ibragimova, A.N. Koval, G.S. Kurskiev, A.E. Litvinov, K.O. Nikolaenko, D.S. Samsonov, V.A. Senichenkov, R.S. Smirnov, S.Y. Tolstyakov, I.B. Tereschenko, L.A. Varshavchik, N.S. Zhiltsov, A.N. Mokeev, P.V. Chernakov, P. Andrew, M. Kempenaars. Fusion Eng. Des. **176**, *9*, 113017 (2022).
[20] G.Y. Sotnikova, A.V. Voronin, V.Y. Goryainov, N.V. Zaitseva, V.N. Klimov, A.V. Nashchekin, R.S. Passet, A.V. Sotnikov. Pis'ma v ZhTF **50**, *3*, 25 (2024) (in Russian).
[21] G.Y. Sotnikova, A.V. Ankudinov, A.V. Voronin, G.A. Gavrilov, A.L. Glazov, V.Yu. Goryainov, N.V. Zaitseva, A.V. Nashchekin, R.S. Passet, A.A. Vorob'ev, A.V. Sotnikov. Ceramics **7**, *4*, 1695 (2024).
[22] V.Yu. Topolov, A.E. Panich. Elektronny nauchny zhurnal „Issledovano v Rossii“ 8 (2008) (in Russian).
[23] A.V.Voronin, V.Yu. Goryainov, V.K. Gusev. ZhTF **90**, *6*, 1028 (2020) (in Russian).
[24] G.Yu. Sotnikova, S.E. Aleksandrov, G.A. Gavrilov. Uspekhi prikladnoi fiziki **10**, *4*, (389) (2022) (in Russian).
[25] A.M. Kosevich. Fizicheskaya mekhanika real'nykh kristallov. Naukova dumka, Kiev (1981). 328 p. (in Russian).
[26] A.A. Skvortsov, O.V. Litvinenko, A.M. Orlov. FTP **37**, *1*, 17 (2003) (in Russian).
[27] A.L. Glazov, K.L. Muratikov. FTT **66**, *36*, 359 (2024) (in Russian).
[28] H.N. Shekhani, E.A. Gurdal, L. Ganapatibhotla, J.K. Maranas, R. Staut, K. Uchino. Material Science **3**, *1*, 10 (2020).

[29] S.N. Kallaev, G.G. Gadzhiev, I.K. Kamilov, Z.M. Omarov, S.A. Sadykov. Izvestiya RAN, ser. fiz. **68**, *7*, 979 (2004) (in Russian).
[30] K.W. Kwok, M.K. Cheung, H.L.W. Chan, C.L. Choy. J. Appl. Phys. **101**, 054108 (2007).
[31] A.K. Tagantsev, I. Stolichnov, E. Colla, N. Setter. J. Appl. Phys. **90**, 1387 (2001).
[32] Q. Huang, Z. Chen, M.J. Cabral, F. Wang, Sh. Zhang, F. Li, Y. Li, Simon P. Ringer, H. Luo, Yiu-Wing Mai, X. Liao. Nat. Commun. **12**, 2095 (2021).
[33] S.B. Lang. Ferroelectrics **118**, *1*, 343 (1991).
[34] S. Biryukov, A. Sotnikov, M. Weihnacht. Ferroelectrics **185**, *1*, 281 (1996).
[35] G.Y. Sotnikova, G.A. Gavrilov, A.A. Kapralov, K.L. Muratikov, E.P. Smirnova. Rev. Sci. Instr. **91**, *1*, 015119 (2020).
[36] N.A. Shvetsova, I.A. Shvetsov, M.A. Lugovaya, E.I. Petrova, A.N. Rybyanets. J. Adv. Dielectr. **12**, *2*, 2160006 (2022).
[37] N.A. Shvetsova, I.A. Shvetsov, E.I. Petrova, A.V. Nasedkin, A.N. Rybyanets. In: *Physics and Mechanics of New Materials and Their Applications. Springer Proceedings in Materials*. Vol. 20. Springer Nature, Switzerland (2023). P. 175.

Translated by T.Zorina